

TeV cosmic-ray proton and helium spectra in the myriad model II

Wei Liu^{1,2}, Pierre Salati³, Xuelei Chen^{1,4}

¹ National Astronomical Observatories, Chinese Academy of Science, Beijing 100012, China

² University of Chinese Academy of Sciences, Beijing 100049, China weiliu@bao.ac.cn

³ LAPTh, Université de Savoie, CNRS, BP 110, 74941 Annecy-le-Vieux, France; salati@lapp.in2p3.fr

⁴ Center of High Energy Physics, Peking University, Beijing 100871, China;
xuelei@cosmology.bao.ac.cn

Received; accepted;

Preprint number LAPTH-026/14

Abstract Recent observations show that the cosmic ray nuclei spectra start to harden above $\sim 10^2$ GeV, in contradiction with the conventional steady-state cosmic ray model. We had suggested that this anomaly is due to the propagation effect of cosmic rays released from local young cosmic ray sources, the total flux of the cosmic ray should be computed with the myriad model, where contribution from sources in local catalogue is added to the background. However, while the hardening could be elegantly explained in this model, the model parameters obtained from the fit skew toward a region with fast diffusion and low supernova rate in the Galaxy, in tension with other observations. In this paper, we further explore this model in order to set up a concordant picture. Two possible improvements related to the cosmic ray sources have been considered. Firstly, instead of the usual axisymmetric disk model, we considered a spiral model of source distribution. Secondly, for the nearby and young sources which are paramount to the hardening, we allow for an energy-dependent escape time. We find that major improvement comes from the energy-dependent escape time of the local sources, and with both modifications, not only the cosmic ray proton and helium anomalies are solved, but also the parameters attain reasonable range values compatible with other analysis.

Key words: catalogs – cosmic rays – pulsars: general

1 INTRODUCTION

It is generally accepted that most of the high energy cosmic ray particles are accelerated in supernova shocks, and form simple power-law spectra $q \propto \mathcal{R}^{-\alpha}$, where $\mathcal{R} \equiv p/Ze$ denotes the rigidity of particle (Axford et al. 1977; Krymskii 1977; Bell 1978; Blandford & Ostriker 1978). After being injected into the interstellar space, the particles are frequently scattered by magnetic irregularities in the Galaxy. This could be described approximately as a diffusion process with spatial diffusion coefficient $K \propto \mathcal{R}^\delta$ (Berezinskii et al. 1990; Maurin et al. 2002b). The diffusion volume is called the magnetic halo. Once the cosmic rays reach a steady state in the halo, the observed cosmic-ray fluxes are given in a large energy range by $\Phi \propto q/K$, i.e. the spectrum scales with energy as a single power law $E^{-(\alpha+\delta)}$, where both α and δ are constant.

Recently the observations of the CREAM (Ahn et al. 2010; Yoon et al. 2011) and PAMELA (Adriani et al. 2011) experiments indicated a hardening of the cosmic nuclei spectra above 250 GeV/nucleon, which extends to TeV energies, though the low energy spectrum measured by the AMS-02 experiment

(AMS-02 2013; Consolandi & on Behalf of the AMS-02 Collaboration 2014) differs somewhat from the PAMELA result, and for the AMS-02 result the hardening is not as significant as the PAMELA one. This problem will be further checked by other experiments, e.g. the AS γ experiment (Tibet AS γ Collaboration et al. 2011; Amenomori et al. 2011) in Yangbajing, Tibet.

A number of different models have been proposed to explain the PAMELA and CREAM anomaly. Most of these focus on the change of energy dependence of either the injection spectrum $q(E)$ (Malkov et al. 2012; Ohira & Ioka 2011; Biernann et al. 2010), or the diffusion coefficient $K(E)$ (Ave et al. 2009; Blasi et al. 2012). A local variation in K proposed by Tomassetti (2012) could induce similar effect. Besides, Blasi & Amato (2012) invokes an unusual strong spallation of the species on the Galactic gas, but this has been criticized by Vladimirov et al. (2012). More recently Thoudam & Hörandel (2013a) considered the diffusive re-acceleration effect, through which the injected energy spectrum can be modified at low energies.

Bernard et al. (2013) proposed that the excess of cosmic-ray nuclei at high energy comes from particular configuration of local sources. To compute the flux of the primary cosmic ray nuclei, instead of the regular steady-state transport model, the myriad-source model (Higdon & Lingenfelter 2003) is employed. In this model the cosmic ray flux is computed in a time-dependent transport framework. For the young and nearby sources, a detailed and complete catalogue was constructed using current survey data, and its contribution was calculated separately. New values of the transport parameters were obtained which fit the proton and helium excess as well as the B/C ratio.

However, although this model could reproduce the observed spectra, it is not completely satisfactory. The best fit model parameters indicates either a thin magnetic halo or a low supernova rate in the Galaxy, but these are in tension with other observations, for example the γ -ray and synchrotron emission (Strong et al. 2010; Bringmann et al. 2012; Di Bernardo et al. 2013). All these results favor a medium size magnetic halo, but for such a halo, e.g. $L \sim 4$ kpc, a low supernova explosion rate is required, at nearly the lower limit of the observations (Diehl et al. 2006). It might be that the contribution from the background sources was overestimated. Another possible problem is that the process for the cosmic ray particles escaping from local supernova remnants (SNRs) was incorrectly modelled.

In this paper we consider two possible improvements to this model. In previous studies (Bernard et al. 2013), we have assumed that the background sources are distributed axisymmetrically in the Galactic disk. In fact, the sources, i.e. supernova remnants are likely distributed along the spiral arms, and to our knowledge the solar system is located between two of them. This difference in the source distribution may affect the result. Moreover, we shall also take the macroscopic size of the local sources and the energy-dependent escape time into account (Thoudam & Hörandel 2012, 2013b). We shall investigate if the fitting to cosmic ray data can be improved, esp. with a higher supernovae explosion rate. We also incorporate the more recent and more precise AMS-02 data (AMS-02 2013; Consolandi & on Behalf of the AMS-02 Collaboration 2014) in our analysis.

The paper is arranged as follows: section 2 and 3 introduce cosmic-ray propagation model and sources respectively. The results are shown in section 4. Finally we give our discussions and conclusions in section 5.

2 COSMIC RAY PROPAGATION MODEL

The galactic supernova explosions which inject cosmic ray particles into the interstellar space can be regarded as a stationary random process. During the average lifetime of the cosmic ray particles the number of supernova explosions is large, as a result a nearly steady average flux is established. However, for short time scales (still large compared with human history) and on scales relevant for observation (solar system), statistical fluctuations can still be large (Bernard et al. 2012), and the contribution of young and nearby sources could result in significant deviation from the average. This could be a possible reason for the observed excess at high energies. To address this possibility, we separate the cosmic ray sources into two components: the remote or aged SNRs which produce a nearly steady background, and the recent and nearby sources which could produce a local deviation in the spectrum. We model the local population by using the information collected from current SNR surveys. Similar ideas were

also explored by [Erlykin & Wolfendale \(2012\)](#) and [Thoudam & Hörandel \(2012\)](#), we expanded it to the whole energy range from tens of GeVs up to a few PeV ([Bernard et al. 2013](#)). The key idea here is that the nearby sources is used to explain the spectral hardening at high energies, whereas the bulk of the remote and old sources account for the fluxes below 250 GeV/nuc. The more energetic particles spend less time in the magnetic halo, making the contribution from local and recent SNRs more important at high energies.

We are interested mainly in the high energy distribution, so diffusive re-acceleration is neglected, as it acts mostly on low energy particles. If we define $\psi \equiv dn/dT$ as the number density per unit volume and unit kinetic energy of a given cosmic ray species, the diffusion equation is

$$\frac{\partial \psi}{\partial t} + \partial_z(V_c \psi) - K(E)\Delta\psi + 2h\delta(z)\Gamma_{\text{sp}}\psi = Q_{\text{acc}}, \quad (1)$$

where V_c is the convective velocity at which cosmic ray particles are blown away from galactic disc by stellar wind. The spatial diffusion coefficient is $K(E) = \kappa_0 \beta \mathcal{R}^\delta$, where κ_0 is a normalization constant and $\beta = v/c$ denotes the particle velocity v in units of speed of light c . Generally the diffusion coefficients form a tensor and are position-dependent, but here for simplicity we assume diffusion to be uniform and isotropic within the magnetic halo. The total cosmic ray flux is $\Phi = v\psi/(4\pi)$. The magnetic halo inside which cosmic ray particles diffuse is assumed to be a flat cylinder, whose thickness $2L$ is an unknown parameter to be determined from fitting to the data. A uniform Galactic disk is located in the middle of halo and its thickness is about 200 pc. The radius of the magnetic halo is usually set to be equal to Galactic radius $R = 20$ kpc. Beyond the magnetic halo, the magnetic field drops rapidly, and the cosmic ray particles are no longer confined. Customarily, at the boundary the freely escape condition is assumed. The last term in the left-hand side of Eq. 1 is the spallation term, with the collision rate Γ given by

$$\Gamma_{\text{sp}} = v(\sigma_{\text{pH}}n_{\text{H}} + \sigma_{\text{pHe}}n_{\text{He}}), \quad (2)$$

in the case of cosmic ray protons. The average densities of hydrogen and helium n_{H} and n_{He} in the disk are 0.9 and 0.1 cm^{-3} respectively. The cross section σ_{pH} is given in [Nakamura & Particle Data Group \(2010\)](#), and σ_{pHe} is assumed to be $4^{2.2/3}\sigma_{\text{pH}}$ ([Norbury & Townsend 2007](#)). For helium cross sections the same scaling factor is adopted.

The sources are assumed to be point-like:

$$Q_{\text{acc}}(\mathbf{x}_S, t_S) = \sum_{i \in \mathcal{P}} q_i \delta^3(\mathbf{x}_S - \mathbf{x}_i) \delta(t_S - t_i). \quad (3)$$

where q_i, \mathbf{x}_i, t_i denote the injection amount, position and time for the i th explosion. For simplicity, we assume q_i to be identical for all the sources and given by

$$q_i^j(p) = q_j^0 \left(\frac{p}{1 \text{ GeV/nuc}} \right)^{-\alpha_j}, \quad (4)$$

for the j th element. The parameters q_j^0 and α_j for proton and helium are determined from parameter fitting. The solution of the transport equation (1) can be written in terms of Green function as

$$\psi(\mathbf{x}, t) = \int_{-\infty}^t dt_S \int_{MH} d^3\mathbf{x}_S \mathcal{G}_p(\mathbf{x}, t \leftarrow \mathbf{x}_S, t_S) Q_{\text{acc}}(\mathbf{x}_S, t_S). \quad (5)$$

The diffusion equation can be solved by numerical integration using the GALPROP([Strong & Moskalenko 1998; Strong et al. 2007](#)) code and its succeeding DRAGON([Evoli et al. 2008; di Bernardo et al. 2010](#)) package. Here we consider another approach, the semi-analytical model([Maurin et al. 2001, 2002a,b](#)). As the diffusion equation is linear, we can write the cosmic ray flux as

$$\Phi = \Phi_{\text{cat}} + \Phi_{\text{ext}}, \quad (6)$$

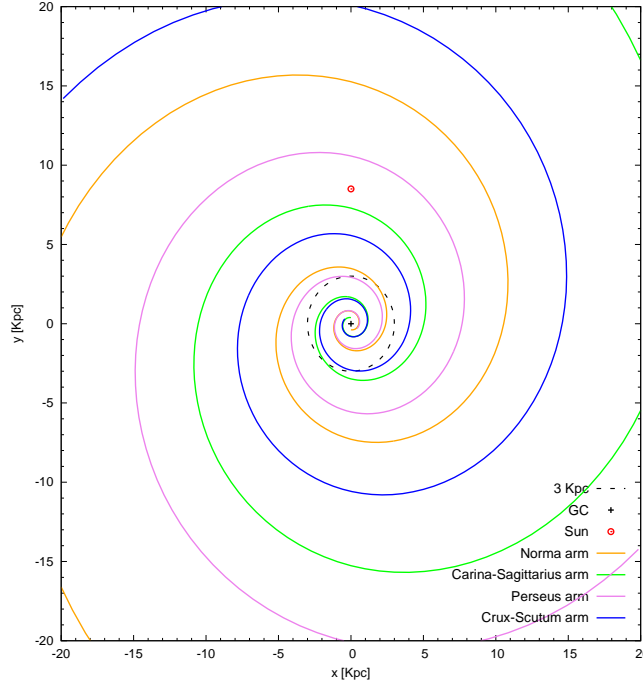


Fig. 1 The Galaxy is assumed to have four spiral arms, with the Sun lying between the Carina-Sagittarius and Perseus arms, about 8.5 kpc away from the Galactic center (Faucher-Giguère & Kaspi 2006).

where Φ_{cat} is the contribution of the nearby and recent sources given in the catalogue, and Φ_{ext} is the flux from the background sources, which can be approximated by its time average $\bar{\Phi}_{\text{ext}}$ (Bernard et al. 2012). The nearby recent supernova explosions can produce fluctuations in cosmic ray fluxes. With data from current surveys, a catalogue of nearby SNRs can be constructed. However, SNRs have limited lifetimes, and faint sources may still be missed. Pulsars are usually regarded as relics of supernova explosions, and are good tracers of aged SNRs. They can be added to known SNRs as a complementary catalogue. A list of cosmic ray sources derived from the Green catalogue (Green 2009) and ATNF pulsar database (Manchester et al. 2005) was presented in Bernard et al. (2013), with the millisecond pulsars associated with known SNRs removed to avoid double counting. In this list, the radial distance extends up to 2 kpc from the Sun, and the upper limit on the age is set to 30,000 years, within which there are 30 sources in total. This is consistent with a supernova explosion rate of 3 per century (Bernard et al. 2012) which could be a local fluctuation on the high side since the Earth is located between two nearby spiral arms.

3 IMPROVEMENTS OF THE SOURCE MODEL

3.1 Spiral distribution of CR sources

Previously the cosmic ray source distribution was usually assumed to be azimuth-symmetric in Galaxy. This is appropriate when the diffusion distance is much larger than the characteristic scale between spiral arms. But when evaluating cosmic ray fluxes at high energies where local sources could play a dominant role, the specific position of the solar system and its local environment may be important.

$$\rho(r) = \left(\frac{r + R_1}{R_\odot + R_1} \right)^a \exp \left[-b \left(\frac{r - R_\odot}{R_\odot + R_1} \right) \right], \quad (7)$$
$$f_i = \frac{1}{\sqrt{2\pi}\sigma} \exp\left(-\frac{(r-r_i)^2}{2\sigma^2}\right) \quad i \in [1, 2, 3, 4] \quad (8)$$

3.2 Energy-dependent escape

According to the diffusive shock acceleration theory, charged particles are accelerated during their repeated crossings of the shock front. They are confined within supernova shock by magnetic turbulence until their upstream diffusion length l_d is larger than the shock radius, which is growing with time. The diffusion length is given by $l_d = D_s/u_s$, where D_s is the diffusion coefficient in the upstream region and u_s is the shock velocity. In the Bohm limit, the diffusion coefficient D_s in the upstream region increases linearly with energy E , $D_s(E) \propto E$. Thus in general the most energetic particles escape from the acceleration region earlier. However the details of how the cosmic ray escape from the source are still not well understood.

$$t_{esc}(\mathcal{R}) = t_{sed} \left(\frac{\mathcal{R}}{\mathcal{R}_{max}} \right)^{-1/\gamma}, \quad (9)$$

where $t_{sed} = 500$ years is the onset time of the Sedov phase, and the maximum rigidity $\mathcal{R}_{max} = 1$ PV. The escape index γ is a positive constant and determines the span of the escape time. When $\gamma \gg 1$,

the escape is very close to instantaneous injection into space. Usually this parameter lies between 1 and 3. When the shock is too weak to accelerate particles and the turbulence level in the upstream region can no longer hold them, the rest of the cosmic ray particles are released all at once. This is assumed to happen at 10^5 years, so the cosmic ray escape time is taken to be

$$T_{esc}(E) = \min(t_{esc}, 10^5 \text{yr}). \quad (10)$$

Along with shock expansion, the shock radius increases according to the Sedov relation

$$R_{esc}(E) = 2.5 u_0 t_{sed} \left\{ \left(\frac{T_{esc}}{t_{sed}} \right)^{0.4} - 0.6 \right\}, \quad (11)$$

where $u_0 = 10^7$ m/s represents the initial velocity of the shock at time t_{sed} . If cosmic rays are assumed to escape from the surface, which is supposed to be spherically symmetric, the source term in equation (1) turns out to be

$$Q(E, t, r) = \frac{q(E)}{A_{esc}} \delta(t - T_{esc}) \delta(r - R_{esc}), \quad (12)$$

where $A_{esc} = 4\pi R_{esc}^2$ is the surface area of the SNR at the escape time T_{esc} , and r denotes the distance to the SNR center.

4 RESULTS

We now try to find the best-fit parameter values by comparing the model prediction on proton and helium spectra with the data from the AMS-02 (AMS-02 2013) and CREAM (Ahn et al. 2010) experiments. We perform the fit in the energy range from 50 GeV/nuc to 100 TeV/nuc, where the solar modulation can be safely neglected. The quality of the fit to the data is analyzed quantitatively by $\chi^2/\text{d.o.f.}$, with the proton and helium data, $\chi^2 = \chi_p^2 + \chi_{He}^2$. Our cosmic ray propagation model is defined by the transport parameters K_0 , δ , V_c and L . All of these are restricted within a range that is consistent with the secondary-to-primary B/C measurements (Maurin et al. 2001). In addition, we have parameters which specify the source properties, including q_p^0 , q_{He}^0 , α_p , α_{He} in Eq.(4), and the average supernova explosion rate ν . Finally, for the energy-dependent escape model, one more parameter, the escape index γ , also needs to be included. The parameters and goodness of fit for the models considered in this paper is listed in Table.1.

In our previous work (Bernard et al. 2013), we studied several configurations, but the supernova explosion rates were close to the lower observational limit, unless L is extremely small. In this paper, we fix the propagation parameters to the MED configuration of Donato et al. (2004); Bernard et al. (2013), where the vertical boundary of halo L has the plausible value of 4 kpc, and also best fits the B/C data (Maurin et al. 2001). We perform a scan over supernova explosion rate, which is required to be larger than 0.8 century^{-1} . Once the transport parameters and the explosion rate are fixed, source parameters q_p^0 , q_{He}^0 , α_p and α_{He} are automatically adjusted to find the best-fit for both proton and helium data.

First, we study the spiral distribution model with instantaneous injection for local sources (model A). The average supernova explosion rate is taken as 0.8 per century . The results are presented in Fig. 2, where the upper curves are for proton, and lower curves for helium. The background sources contribution Φ_{ext} is plotted as the green dotted lines, the nearby young sources contribution Φ_{cat} as the purple dash-dotted lines, and the total flux as the blue solid lines. The background flux Φ_{ext} is dominant below ~ 100 GeV, where the AMS-02 data dominate the fit. As energy increases, the background contribution shrinks, while the contribution from nearby young sources raises.

As shown in Table.1, we find that compared with the original axisymmetric model (Bernard et al. 2013), the goodness of fit for the spiral model is not improved. To understand this, in Fig. 3 we compare the proton flux for models A (spiral) with model Aa (axi-symmetric). Both models are based on the

Table 1 The sets of cosmic ray injection and propagation parameters and the goodness of fit for different models considered in this paper. The Aa (axisymmetric) and A(spiral) models assume point sources and instantaneous injection, while the B,C,D and E models include effects of finite size and energy-dependent escape. The index γ specifies energy-dependence of escape time (see Eq.(9)).

Model	A	Aa	B	C	D	E
Diffusion coefficient normalization K_0	0.0112	0.0112	0.0112	0.0112	0.0112	0.0112
Diffusion spectral index δ	0.7	0.7	0.7	0.7	0.7	0.7
Magnetic halo half thickness L [kpc]	4	4	4	4	4	4
Convective Velocity V_c [km s $^{-1}$]	12	12	12	12	12	12
SN explosion rate ν [century $^{-1}$]	0.8	0.8	1.2	1.4	1.7	1.5
SN proton injection number g_p^0 [10^{52} GeV $^{-1}$]	2.527	1.773	1.355	1.188	0.933	1.068
SN proton spectral index α_p	2.2	2.17	2.154	2.159	2.150	2.151
SN helium injection number g_{He}^0 [10^{51} GeV $^{-1}$]	1.475	1.044	0.768	0.734	0.554	0.648
SN helium spectral index α_{He}	2.07	2.04	2.012	2.037	2.017	2.024
Energy-dependence index γ	∞	∞	2	3	2.36	2.37
Goodness of Fit χ^2/dof	2.19	1.93	1.708	1.552	1.751	1.469

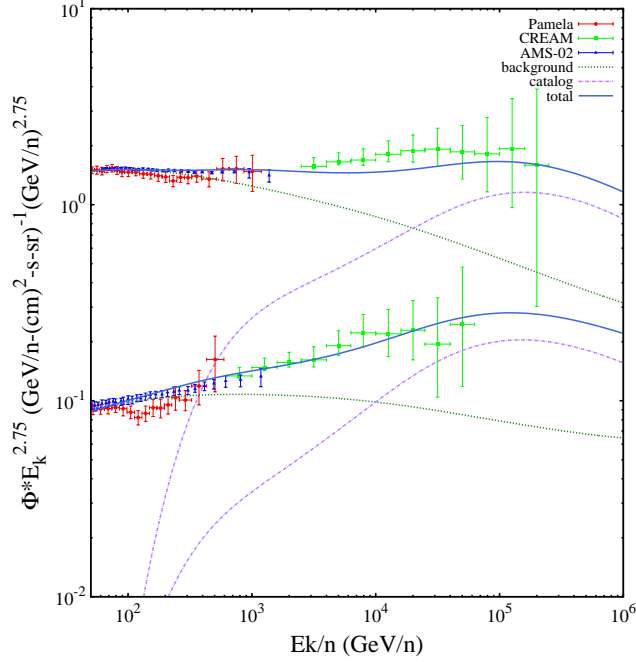


Fig. 2 The best-fit model A(see table 1) to the AMS-02 and CREAM data under spiral distribution of background sources, where local sources are assumed to be point-like with instantaneous injection. The propagation parameters are configured to the MED case, where L is 4 kpc, and explosion rate of 0.8 per century is assumed. Proton(upper curve) and helium(lower curve) spectra are featured in the energy range extending from 50 GeV/nuc to 100 TeV/nuc. The contribution from the background sources corresponds to the green dotted lines. The blue solid lines show the total flux while the purple dash-dotted curves indicate the flux from the sources of the catalog.

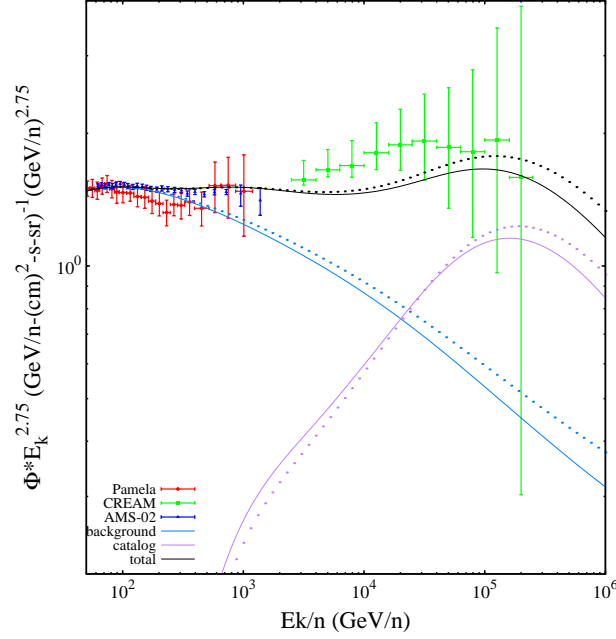


Fig. 3 Various contributions to the proton flux have been calculated in the spiral and axisymmetric source models for comparison purposes. The solid and dotted curves correspond to the spiral and axisymmetric configurations A and Aa of Table 1 respectively. The black lines feature the total flux which is a sum of the contributions from the background sources (blue) and from the catalog of local objects (purple).

same cosmic ray propagation parameters, and have the same average supernova explosion rate ν . The solid curves correspond to the spiral model A whereas the dotted curves feature the axisymmetric case model Aa. For the low energy part, the two models have almost the same background contribution. Now the Earth is located between the Carina-Sagittarius and Perseus arms, the number of sources which contribute to Φ_{ext} are less numerous in the spiral model than for the axisymmetric model. The latter tends to overpopulate the void inside which the solar system is located and leads to a slightly larger background flux above ~ 1 TeV. This effect is counterbalanced by a smaller contribution Φ_{cat} from the local sources up to an energy of 10 TeV, so the best-fit value for q_p^0 is larger in model A than in model Aa. Conversely, the high-energy data points demands a slightly softer injection spectrum and a larger value for the index α_p in model A than Aa. However, the difference between model A and model Aa is not very significant. Perhaps more important is the behavior of the background flux Φ_{ext} at high energy in the presence of spiral arms, as the energy increases, it drops faster than the simple power-law as was assumed in Thoudam & Hörandel (2012, 2013b).

Next we consider the energy-dependent injection from local sources, the background sources are assumed to be spirally distributed. As we discussed earlier, modifying the escape index γ changes the energy range where the local component comes into play. When γ gets large, energy-dependent escape gradually approaches an instantaneous injection taking place at the start of the Sedov phase, and sources then behave as point-like objects (the radius is only ~ 5 pc). As γ decreases, the span of escape time becomes longer. The most energetic particles escape first from the SNR. When the injection timescale becomes comparable with the upper limit of 30,000 years on the age of the local sources, only the most energetic cosmic rays are released and make it to Earth. We explored different values of γ , and found at γ values at $2 \sim 3$ good fits can be obtained. In the best-fit models B and C, the MED propagation

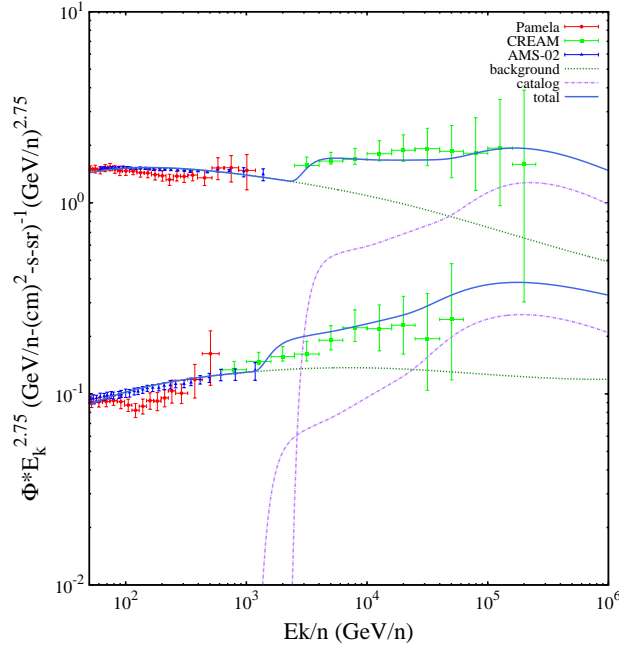


Fig. 4 Model B assumes energy-dependent escape of cosmic rays from local sources. The escape index γ is set equal to 2 as default value while the explosion rate is equal to 1.2 per century. The cosmic ray propagation parameters are configured to the MED model.

parameters are assumed, with $\gamma = 2$ and $\gamma = 3$ for model B and C, respectively. We explore here how the local flux Φ_{cat} reacts to a change in the escape index γ . The results are shown in Figs. 4 and 5. There is a low energy cut-off in the local contributions to the proton and helium fluxes in the case of model B where $\gamma = 2$ has been assumed. This is due to the energy-dependent cosmic ray release mechanism we discussed earlier: the lower energy cosmic ray particles from young sources have not yet been released or reached Earth. As a result of this low energy cut-off, there is also a kink at this energy in the spectrum predicted by the model. In model C, with $\gamma = 3$, the cutoff is not as sharp and the local flux starts to contribute from lower energies. The kink in total flux at low energy in model B (Fig. 4) disappeared in model C (Fig. 5).

We find that when taking the energy-dependent escape into account, the goodness of fit is markedly improved. For completeness, we have also varied the supernova explosion rate between models B and C. A larger value of ν translates into a larger abundance of sources contributing to the overall signal. The amount of cosmic rays injected by a single object decreases as is clear shown in Table 1. Although the effect is marginal, the contribution from local sources drops gradually with increasing explosion rate.

Finally, we consider the injection index γ as a free parameter and let it vary between 2 and 3. Model D (Fig. 6) and Model E (Fig. 7) is for SN explosion rates of 1.7 and 1.5 per century, respectively. These values are very close to the average determined by Diehl et al. (2006). Further increasing the explosion rate would make fitting worse, especially for the proton spectrum.

5 CONCLUSION

The spectral hardening exhibited by the cosmic ray proton and helium fluxes above a few hundreds of GeV/nuc in the PAMELA (Adriani et al. 2011) data is no longer present in the AMS-02 (AMS-02 2013) observations which point toward a power-law behavior. But the CREAM (Ahn et al. 2010; Yoon

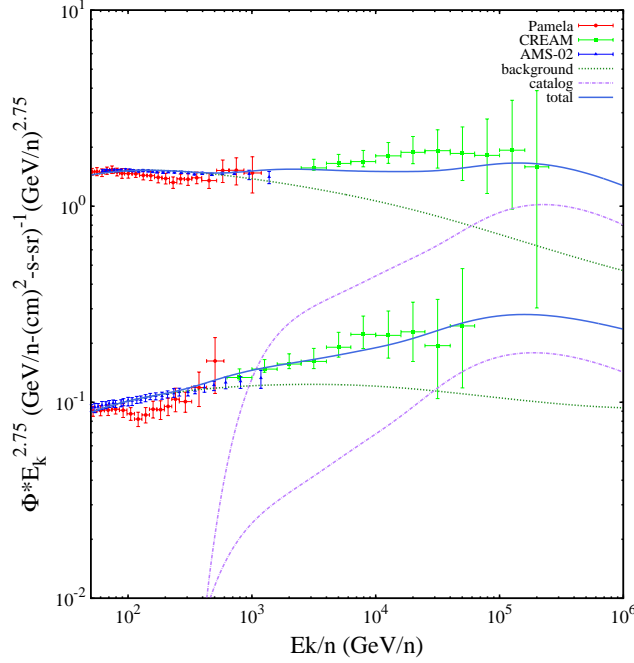


Fig. 5 Another best-fit model C with same constraints as before. The escape index γ is set equal to 3 as default value and the explosion rate is equal to 1.4 per century.

et al. 2011) experiment still reports an excess above ~ 1 TeV/nuc which is hard to understand in the conventional model of cosmic ray transport and the problem persists. We propose here a solution in terms of the known local and young SNRs whose contributions become dominant above TeV energies. These sources have been extracted from astronomical catalogs. The cosmic ray transport model has also been set to the MED configuration which best-fits the B/C ratio. The thickness of the diffusive halo is 4 kpc, a value that has been so far considered as canonical.

In this paper, we have improved over our previous analysis in three respects. To commence, we have used the AMS-02 data which are much more difficult to accommodate with a TeV spectral hardening than the PAMELA observations. The goodness of our fits suffers from the power-law behavior of the AMS-02 measurements as well as from smaller error bars associated with a significant improvement in the accuracy of the data. In spite of this, we get reduced chi-square values which are still satisfactory. To do so, we have introduced two major revisions for the sources of our model. Supernova explosions are distributed along spiral arms as they should in a typical SBc galaxy as the Milky Way. The previous axi-symmetric distribution of CR background sources has thus been replaced by a spiral distribution. Then, we have explicitly taken into account the finite size of the local sources, for which this effect is the most severe, and we have also modelled the energy-dependent escape of cosmic rays from them.

We find that considering a spiral distribution for the background CR sources only leads to limited improvements. On the contrary, a better description of local sources induces obvious effects. For the canonical MED model of CR transport parameters, the average explosion rate ν can be as large as 1.5 per century, or even 1.7 for model D, and becomes close to the fiducial value of 1.9 ± 1.1 found by Diehl et al. (2006). This is a significant improvement over the Bernard et al. (2013) analysis where ν had to be as small as 0.8 per century, with a reduced chi-square value of 1.3 based on the PAMELA data, to be compared to our best-fit result of 1.47 obtained with the more constraining AMS-02 measurements. We confirm that a higher explosion rate reduces the role of local sources as is clear in Table 1 where

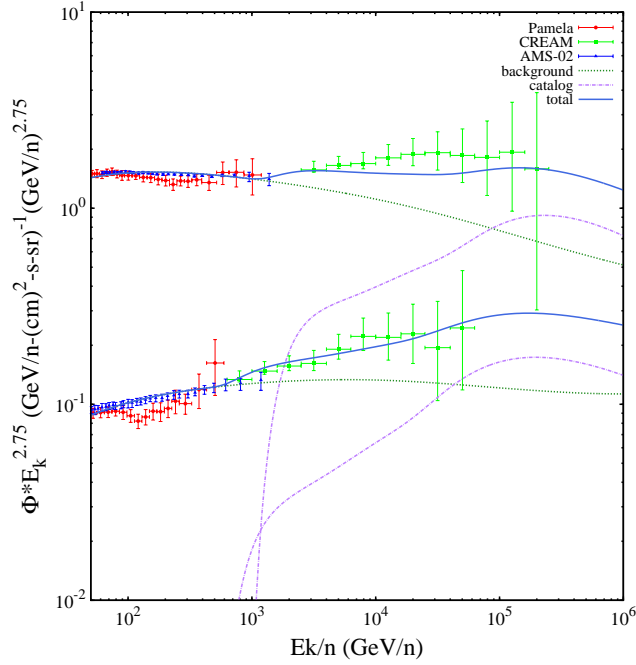


Fig. 6 The best-fit model D is obtained by setting the explosion rate ν equal to 1.7 per century and by letting the escape index γ vary between 2 and 3. The latter adjusts itself to a value of 2.36 close to 2, hence a kink in the proton and helium spectra at $\sim 1 \text{ TeV/nuc}$.

the proton and helium yields q_p^0 and q_{He}^0 are anti-correlated with ν . Our best-fit models D and E feature a characteristic kink at a few TeV/nuc. Should this hardening be confirmed by future observations, it would point toward sources where the release of cosmic rays in interstellar space cannot be considered as instantaneous, the most energetic particles being emitted first.

Acknowledgements This work is supported by the Ministry of Science and Technology 863 project 2012AA121701, by the Chinese Academy of Science Strategic Priority Research Program “The Emergence of Cosmological Structures” of the Chinese Academy of Sciences, Grant No. XDB09000000, and the NSFC grant 11373030. This work has also been supported by Institut universitaire de France.

References

- Adriani, O., Barbarino, G. C., Bazilevskaya, G. A., et al. 2011, *Science*, 332, 69 [1](#), [9](#)
Ahn, H. S., Allison, P., Bagliesi, M. G., et al. 2010, *ApJ*, 714, L89 [1](#), [6](#), [9](#)
Amenomori, M., Bi, X. J., Chen, D., et al. 2011, *Astrophysics and Space Sciences Transactions*, 7, 15 [2](#)
AMS-02 2013, <http://www.ams02.org/>, [Online] [2](#), [6](#), [9](#)
Ave, M., Boyle, P. J., Höppner, C., Marshall, J., & Müller, D. 2009, *ApJ*, 697, 106 [2](#)
Axford, W. I., Leer, E., & Skadron, G. 1977, in *International Cosmic Ray Conference, International Cosmic Ray Conference*, vol. 11, 132–137 [1](#)
Bell, A. R. 1978, *MNRAS*, 182, 147 [1](#)
Berezinskii, V. S., Bulanov, S. V., Dogiel, V. A., & Ptuskin, V. S. 1990, *Astrophysics of cosmic rays* [1](#)
Bernard, G., Delahaye, T., Keum, Y.-Y., et al. 2013, *A&A*, 555, A48 [2](#), [3](#), [4](#), [6](#), [10](#)
Bernard, G., Delahaye, T., Salati, P., & Taillet, R. 2012, *A&A*, 544, A92 [2](#), [4](#)

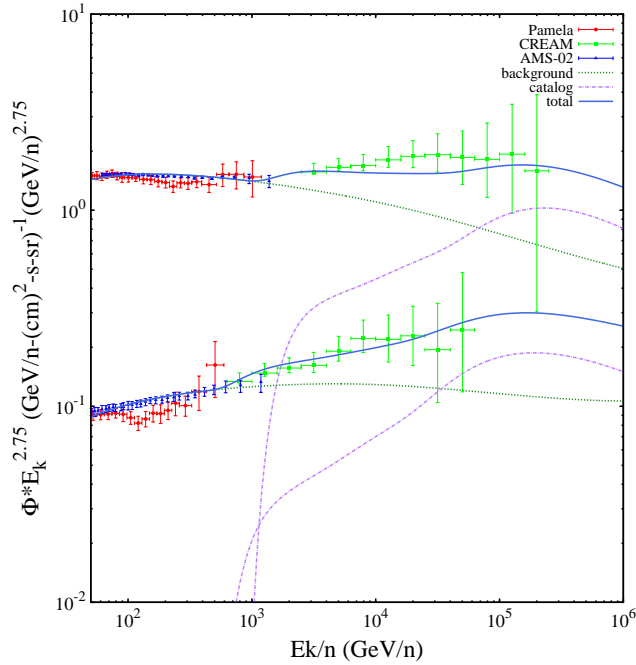


Fig. 7 The previous fit is improved in model E where the explosion rate ν is now decreased to a value of 1.5 per century.

- Biermann, P. L., Becker, J. K., Dreyer, J., et al. 2010, *ApJ*, 725, 184 [2](#)
- Blandford, R. D., & Ostriker, J. P. 1978, *ApJ*, 221, L29 [1](#)
- Blasi, P., & Amato, E. 2012, *J. Cosmology Astropart. Phys.*, 1, 010 [2](#), [5](#)
- Blasi, P., Amato, E., & Serpico, P. D. 2012, *Physical Review Letters*, 109, 061101 [2](#)
- Bringmann, T., Donato, F., & Lineros, R. A. 2012, *J. Cosmology Astropart. Phys.*, 1, 049 [2](#)
- Consolandi, C., & on Behalf of the AMS-02 Collaboration 2014, *ArXiv e-prints* [2](#)
- di Bernardo, G., Evoli, C., Gaggero, D., Grasso, D., & Maccione, L. 2010, *Astroparticle Physics*, 34, 274 [3](#)
- Di Bernardo, G., Evoli, C., Gaggero, D., Grasso, D., & Maccione, L. 2013, *J. Cosmology Astropart. Phys.*, 3, 036 [2](#)
- Diehl, R., Haloin, H., Kretschmer, K., et al. 2006, *Nature*, 439, 45 [2](#), [9](#), [10](#)
- Donato, F., Fornengo, N., Maurin, D., Salati, P., & Taillet, R. 2004, *Phys. Rev. D*, 69, 063501 [6](#)
- Effenberg, F., Fichtner, H., Scherer, K., & Büsching, I. 2012, *ArXiv e-prints* [5](#)
- Elmegreen, D. M. 1998, *Galaxies and galactic structure* [5](#)
- Erlykin, A., & Wolfendale, A. 2012, *Astroparticle Physics*, 35, 371 [3](#)
- Evoli, C., Gaggero, D., Grasso, D., & Maccione, L. 2008, *J. Cosmology Astropart. Phys.*, 10, 018 [3](#)
- Faucher-Giguère, C.-A., & Kaspi, V. M. 2006, *ApJ*, 643, 332 [4](#), [5](#)
- Gaggero, D., Maccione, L., Di Bernardo, G., Evoli, C., & Grasso, D. 2013, *Physical Review Letters*, 111, 021102 [5](#)
- Green, D. A. 2009, *Bulletin of the Astronomical Society of India*, 37, 45 [4](#)
- Higdon, J. C., & Lingenfelter, R. E. 2003, *ApJ*, 582, 330 [2](#)
- Krymskii, G. F. 1977, *Akademiia Nauk SSSR Doklady*, 234, 1306 [1](#)
- Malkov, M. A., Diamond, P. H., & Sagdeev, R. Z. 2012, *Physical Review Letters*, 108, 081104 [2](#)
- Manchester, R. N., Hobbs, G. B., Teoh, A., & Hobbs, M. 2005, *AJ*, 129, 1993 [4](#)

- Maurin, D., Donato, F., Taillet, R., & Salati, P. 2001, *ApJ*, 555, 585 [3](#), [6](#)
- Maurin, D., Taillet, R., & Donato, F. 2002a, *A&A*, 394, 1039 [3](#)
- Maurin, D., Taillet, R., Donato, F., et al. 2002b, *ArXiv Astrophysics e-prints* [1](#), [3](#)
- Nakamura, K., & Particle Data Group 2010, *Journal of Physics G Nuclear Physics*, 37, 075021 [3](#)
- Norbury, J. W., & Townsend, L. W. 2007, *Nuclear Instruments and Methods in Physics Research Section B: Beam Interactions with Materials and Atoms*, 254, 187 [3](#)
- Ohira, Y., & Ioka, K. 2011, *ApJ*, 729, L13 [2](#)
- Shaviv, N. J. 2002, *Physical Review Letters*, 89, 051102 [5](#)
- Shaviv, N. J. 2003, *New Astronomy*, 8, 39 [5](#)
- Shaviv, N. J., Nakar, E., & Piran, T. 2009, *Physical Review Letters*, 103, 111302 [5](#)
- Strong, A. W., & Moskalenko, I. V. 1998, *ApJ*, 509, 212 [3](#)
- Strong, A. W., Moskalenko, I. V., & Ptuskin, V. S. 2007, *Annual Review of Nuclear and Particle Science*, 57, 285 [3](#)
- Strong, A. W., Porter, T. A., Digel, S. W., et al. 2010, *ApJ*, 722, L58 [2](#)
- Thoudam, S., & Hörandel, J. R. 2012, *MNRAS*, 421, 1209 [2](#), [3](#), [5](#), [8](#)
- Thoudam, S., & Hörandel, J. R. 2013a, *ArXiv e-prints* [2](#)
- Thoudam, S., & Hörandel, J. R. 2013b, *ArXiv e-prints* [2](#), [5](#), [8](#)
- Tibet As γ Collaboration, Amenomori, M., Bi, X. J., et al. 2011, *Advances in Space Research*, 47, 629 [2](#)
- Tomassetti, N. 2012, *ApJ*, 752, L13 [2](#)
- Vallée, J. P. 1995, *Astrophysical Journal*, 454, 119 [5](#)
- Vallée, J. P. 2002, *Astrophysical Journal*, 566, 261 [5](#)
- Vladimirov, A. E., Jóhannesson, G., Moskalenko, I. V., & Porter, T. A. 2012, *ApJ*, 752, 68 [2](#)
- Yoon, Y. S., Ahn, H. S., Allison, P. S., et al. 2011, *ApJ*, 728, 122 [1](#), [9](#)
- Yusifov, I., & Küçük, I. 2004, *A&A*, 422, 545 [5](#)